Electronic Supplementary Material (ESI) for ChemComm.

Supplementary Information

All-graphene oxide device with tunable supercapacitor and battery behaviour by the working voltage

Chikako Ogata,*[a] Ruriko Kurogi,[a] Kazuto Hatakeyama,[a] Takaaki Taniguchi, [b] Michio Koinuma[a] and Yasumichi Matsumoto*[a]

[a] Graduate School of Science and Technology Kumamoto University, 2-39-1 Kurokami, Chuo-ku, Kumamoto 860-8555, Japan

[b] International Center for Materials Nanoarchitectonics (WPI-MANA), National Institute for Materials Science (NIMS), 1-1 Namiki, Tsukuba, Ibaraki 305-0044, Japan

Corresponding Author

124d9201@st.kumamoto-u.ac.jp (Chikako Ogata)

yasumi@gpo.kumamoto-u.ac.jp (Yasumichi Matsumoto)

Experimental Section

1. Synthesis of graphene oxide

The graphene oxide (GO) was prepared from natural graphite powder (special grade reagent, Wako Ltd.) by Hummers' method.[1] Graphite powder (2.0 g), $NaNO_3$ (2 g, special reagent, Wako Ltd.) and 98% H_2SO_4 (92 mL, special reagent, Wako Ltd.) were mixed at 0 °C in an ice-water bath. $KMnO_4$ (12 g, special reagent, Wako Ltd.) was added slowly. The reaction mixture was removed from the ice-water bath and stirred to oxidise the graphite powder for 45 min at 95 °C. The resulting mixture was diluted with distilled water, and 30% H_2O_2 (5 mL, special reagent, Wako Ltd.) was added to neutralise any remaining $KMnO_4$. The product was washed with 5% HCl (special reagent, Wako Ltd.), centrifuged several times at 3,000 rpm to remove excess HCl and dried in an oven at 70 °C for 7 days. GO was suspended in distilled water by bath sonication for 2 h, and the resulting suspension was ultracentrifuged at 10,000 rpm. The supernatant was used as the GO suspension.

2. Preparation of GO paper

The GO suspensions (4 mg mL^{-1}, 20 mL) were filtered using a membrane filter (0.4 μm pore size, Merck Millipore) under reduced pressure overnight and then peeled from the filter, resulting in free-standing and flexible GO paper.

3. Fabrication of reduced GO/GO/ reduced GO devices

The reduced GO (rGO)/GO/rGO structure was fabricated by photoirradiation of both surfaces of the GO paper for 1 to 12 h in air using a 500 W (32.5 mW cm^{-2}) high-pressure mercury lamp (USHIO, SX-U1501HQ). Au was sputter-coated onto both surfaces of the rGO/GO/rGO film using a sputtering machine (K575K, Emitech) to improve the contact. Photoreduction and Au sputtering were performed using a mask to define the electrode area (diameter circle: 1 cm).

4. Characterisation

The morphology of the samples was verified using field-emission scanning electron microscope (FE-SEM; Hitachi High-Tech, SU-8000). X-ray photoelectron spectroscopy (XPS, Thermo Scientific, Sigma Probe) was used to determine the degree of oxidation of the samples. Thermogravimetric analysis (TGA) curves were generated using a thermal analyser (Seiko Instruments, EXSTAR 6000). The experiments were designed from room temperature to 1,000 °C at a heating rate 4 °C min^{-1} under nitrogen protection. To exclude the moisture desorption below 100 °C, the obtained results were analysed above that temperature.[2]

5. Electrochemical characterisation of rGO/GO/rGO devices

The electrochemical performance of the rGO/GO/rGO devices was investigated using cyclic voltammetry (CV), galvanostatic charge/discharge (CC) measurements and electrochemical impedance spectroscopy (EIS). CV and CC measurements were performed on an electrochemical workstation (IVIUM TECHNOLOGIES, CompactStat). EIS measurements were recorded on an impedance/gain phase analyser (Solartron 1260) over the frequency range from 2 MHz to 0.01 Hz with an amplitude of 50 mV. All experiments were performed at 25 °C 40% after being maintained for 1 h under ambient conditions to become stable.

6. Calculations

6.1. Capacitance

The capacitance was calculated from the CV and CC data according to the following formula:

$$C_{device} = \frac{I}{dV/dt},$$

where *I* refers to the mean current in the CV curves and the set current in CC, and *dV/dt* refers to the scan rate in the CV curves or to the slope of the discharge curves in CC.

Specific capacitances were calculated on the basis of the area or the volume of the device stack according to the following formulas:

$$Areal\ capacitance\ = \frac{C_{device}}{A}\ ,$$

$$Volumetric\ stack\ capacitance\ = \frac{C_{device}}{V}\ ,$$

where A refers to the total surface area (cm^2) of the positive and negative electrode and V refers to the volume (cm^3) of the device. The stack capacitances (F cm^{-3}) were calculated with the volume of the device taken into account, including the rGO, GO and Au current collector. The rGO electrodes were typically circular, with a diameter of 1 cm. In the rGO/GO/rGO devices, A was $2 \times 0.5^2 \times \pi$ (cm^2) and V was $0.5^2 \times \pi \times$ thickness of the rGO/GO/rGO device (cm^3).

The power density of the devices was calculated from the galvanostatic curves at different CC current densities using the following formula:

$$P_{max} = \frac{\Delta E^2}{4R_{ESR}V}\ ,$$

where P is the power density (W cm^{-3}), ΔE is the operating voltage window (measured in volts and obtained from the discharge curve excluding the IR drop) and V is the volume of the device as indicated earlier (in cm^3). Parameter R_{ESR} is the internal resistance of the device, which was estimated from the voltage drop at the beginning of the discharge, V_{drop}, at a constant current density (i) using the equation

$$R_{ESR} = \frac{V_{drop}}{2i}\ .$$

The energy density of the device was obtained from the formula

$$E = \frac{C_V \times \Delta E^2}{2 \times 3600}\ ,$$

where E is the energy density (Wh cm^{-3}), C_V is the volumetric stack capacitance and ΔE is the operating voltage window in volts (measured in volts and obtained from the discharge curve, excluding the IR drop).

6.2. Mass of rGO electrode

Assuming that there is no involvement of other types of elements (such as hydrogen, 2H + O → H_2O) and that two oxygen atoms will react with one carbon atom to de-functionalise at a high temperature,

$$C + 2O \rightarrow CO_2$$

According to XPS results, the atomic ratio of oxygen is 39%, the atomic ratio of carbon is 61%, and all oxygen leaves the sample in the form of carbon dioxide. Thus,

$$Wt\%_{left} = 1 - Wt\%_{burned} = 1 - \frac{weight_{burn}}{weight_{starting}}$$

$$= 1 - \frac{weight_{carbonburned} + weight_{oxygenburned}}{weight_{carbonstarting} + weight_{oxygenstarting}}$$

$$= 1 - \frac{\left(\frac{0.39}{2}\right) \times 12\ g \cdot mol^{-1} + 0.39 \times 16\ g \cdot mol^{-1}}{0.61 \times 12\ g \cdot mol^{-1} + 0.39 \times 16\ g \cdot mol^{-1}}$$

$$= 36.73\ wt\%$$

TGA measurement reveals that 35.77 wt% is left of the GO film, which is close to the calculated value of 36.73 wt%.

Similarly, according to XPS results, the atomic oxygen ratio is 23% for the rGO external layer. Thus,

$$Wt\%_{left} = 1 - Wt\%_{burned} = 1 - \frac{weight_{burn}}{weight_{starting}}$$

$$= 1 - \frac{weight_{carbonburned} + weight_{oxygenburned}}{weight_{carbonstarting} + weight_{oxygenstarting}}$$

$$= 1 - \frac{\left(\frac{0.23}{2}\right) \times 12\ g \cdot mol^{-1} + 0.23 \times 16\ g \cdot mol^{-1}}{0.77 \times 12\ g \cdot mol^{-1} + 0.23 \times 16\ g \cdot mol^{-1}}$$

$$= 60.84\ wt\%$$

Therefore, after de-functionalisation at high temperature in TGA, assuming that the sandwiched GO film is with α wt% of rGO external layers and (100 − α) wt% of GO intralayers, the percentage P of left weight can be calculated as

$$P = \alpha\ wt\% \times 60.84\ wt\% + (1 - \alpha\ wt\%) \times 36.73, and\ P = 36.75\ wt\%$$

Thus, rGO external layers occupy a weight percentage α wt% = 0.8 wt% in GOSC-6 h.

7. Electron conductivity measurement of GO and rGO films

The electron conductivities of the samples were measured by a four-probe DC method using an electrochemical workstation (IVIUM TECHNOLOGIES, CompactStat). The four-probe measurement with a BT-115 conductivity cell (ElectroChem, Inc.) was performed on a single piece of GO film with a thickness of 50 μm. The spacing between each probe was 0.5 cm, and the length of each probe was 2.0 cm.

The corresponding electron conductivity was calculated from the resistance value according to the following formula:

$$\sigma = \frac{d}{R \times T \times L},$$

where σ is the electron conductivity, d is the width (the distance between the electrodes, 0.5 cm), R is the resistance value in Ω obtained from the *I–V* curve, T is the thickness of the GO film in cm and L is the length of the membrane (1 cm). The calculated electron conductivity is expressed in units of S cm^{-1}.

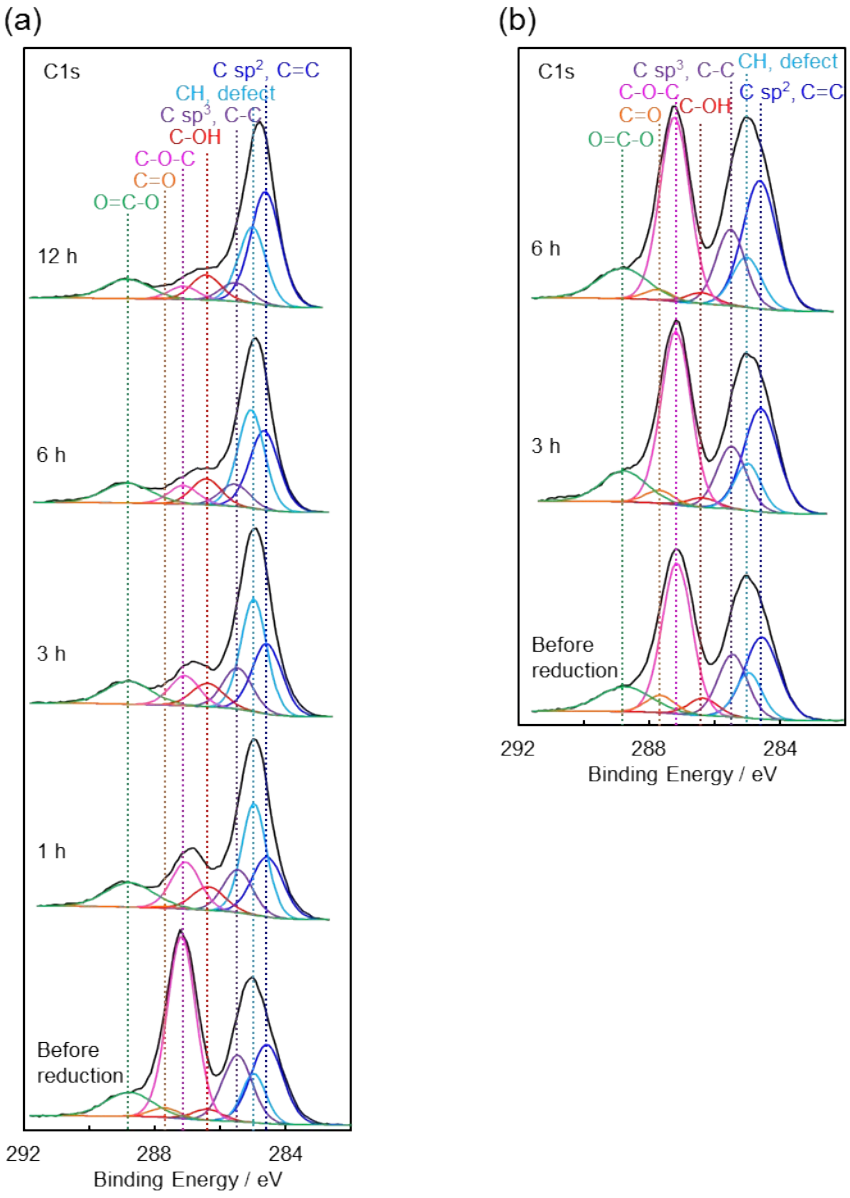

Figure S1. C 1s XPS spectra of (a) surface and (b) interlayer of rGO/GO/rGO at various photoreduction times. The interlayer of rGO/GO/rGO was obtained by peeling off the rGO layer using scotch tape. The C 1s XPS spectra were split into seven groups (–COOH, C=O, C–O–C, C–OH, sp^3 C–C, C–H defect and sp^2 C=C bonds) according to our previous report.[3]

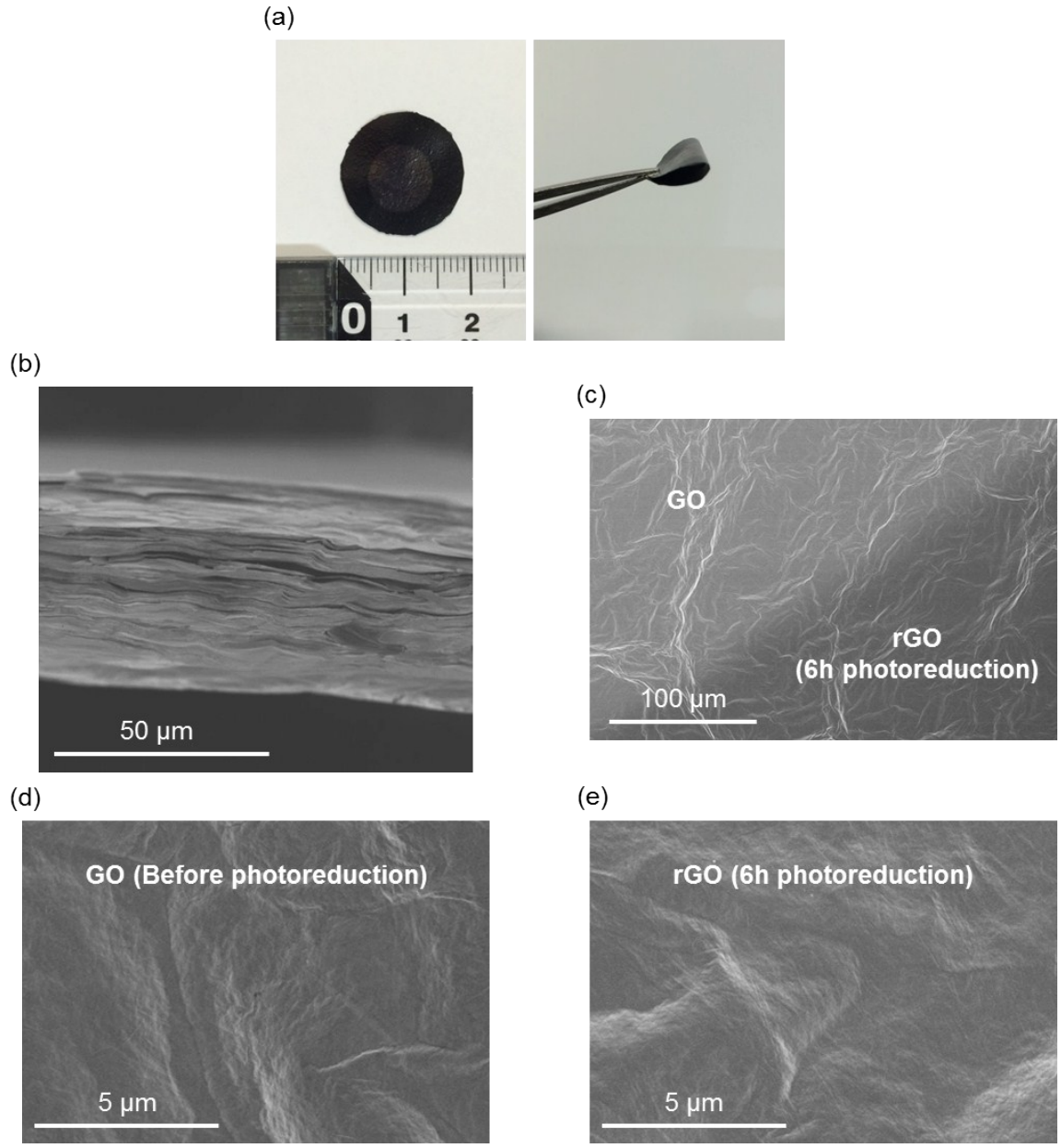

Figure S2. (a) A digital photograph of the rGO/GO/rGO device. (b) Cross-sectional SEM image of rGO/GO/rGO constructed with a photoreduction time of 6 h. Analysis of the cross section of this device reveals a thickness of approximately 50 μm. (c-d) Different magnification SEM images of GO/rGO boundary of the surface, GO surface and rGO surface. Because photoreduction was not associated with thermal effects,[2,4,5] the morphological change between GO and rGO was not observed clearly.

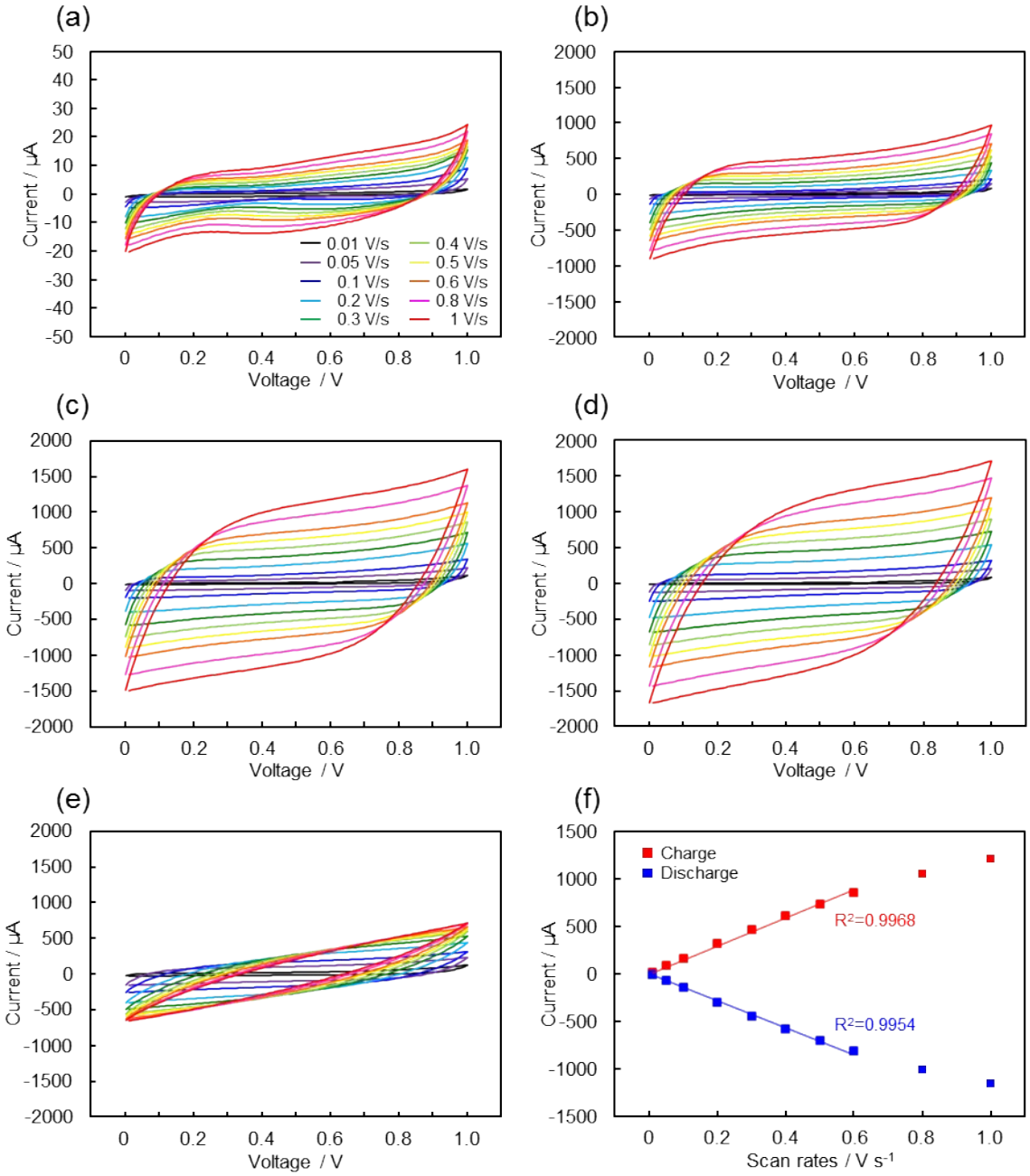

Figure S3. CV profiles of GOSC at various scan rates, where the GOSC samples were prepared using various photoreduction times: (a) Before photoreduction, (b) GOSC-1 h, (c) GOSC-3 h, (d) GOSC-6 h and (d) GOSC-12 h. (f) Dependence of the capacitive current (extracted from the CV profiles at 0.5 V) of GOSC-6 h in the applied scan rate between 10 to 1,000 mV s^{-1}. A linear relationship is observed with R^2 = 0.9968 and 0.9954 for the charge and discharge curves at least up to 600 mV s^{-1}, respectively. In contrast to our GOSC-6 h, GO-based micro-supercapacitor exhibits the desired rectangular CV shape only at slow scan rates, 2 to 200 mV s^{-1},[2,5] indicating the limited rate performance of this supercapacitor.

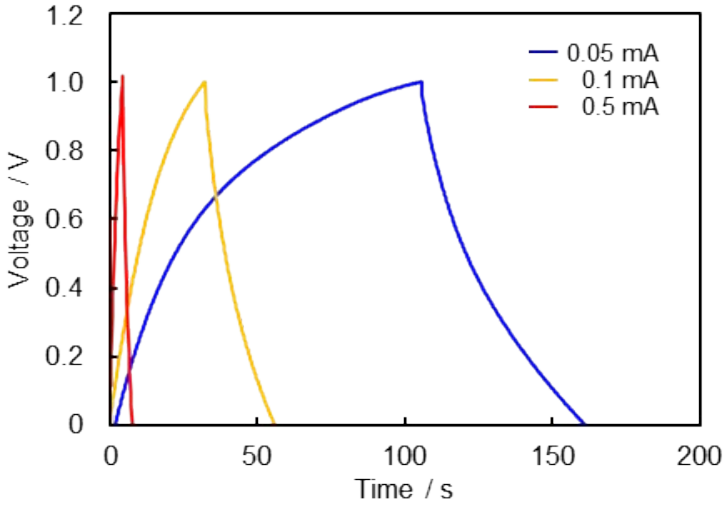

Figure S4. Galvanostatic charge/discharge curves of GOSC-6 h collected at different current densities. The specific capacitances of the samples were 2.1 (0.05 mA), 1.7 (0.1 mA) and 1.3 mF cm^{-2} (0.5 mA).

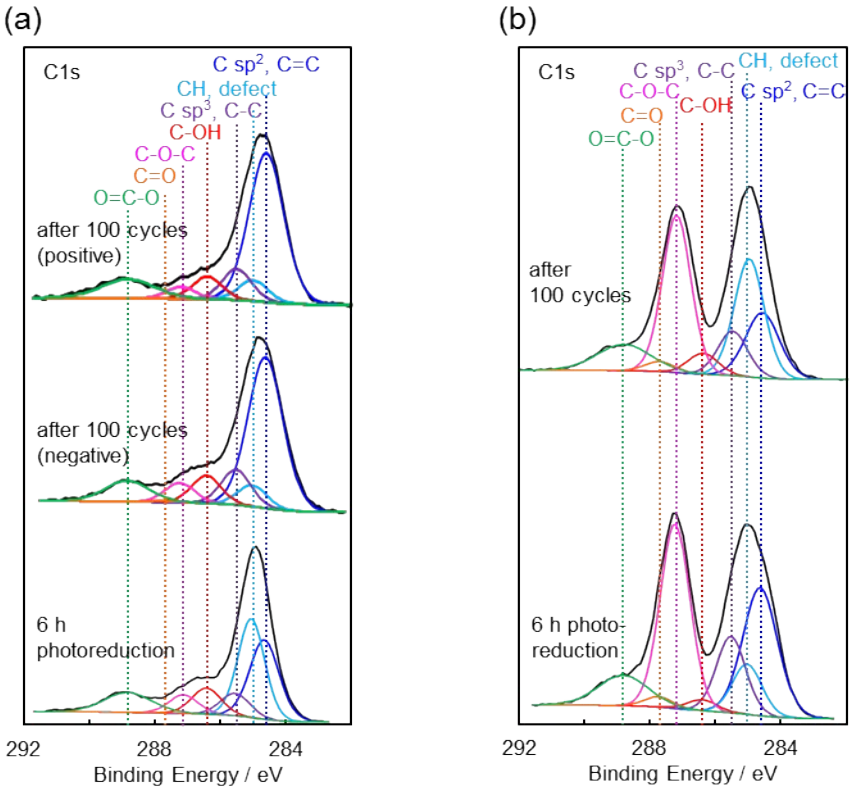

Figure S5. C 1s XPS spectra of (a) rGO electrode and (b) GO interlayer of GOSC-6 h before and after charge/discharge cycles. The interlayer of GOSC-6 h was obtained by peeling off the rGO layer using scotch tape.

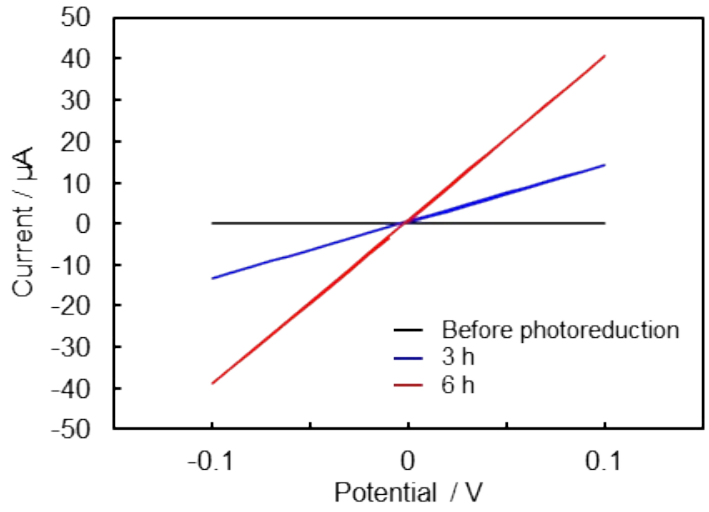

Figure S6. Typical *I*–*V* curves of GO and rGO films prepared at various photoreduction times. The electron conductivities were 2.04×10^{-9} (before photoreduction), 1.41×10^{-2} (3 h) and 4.03×10^{-2} S cm^{-1} (6 h).

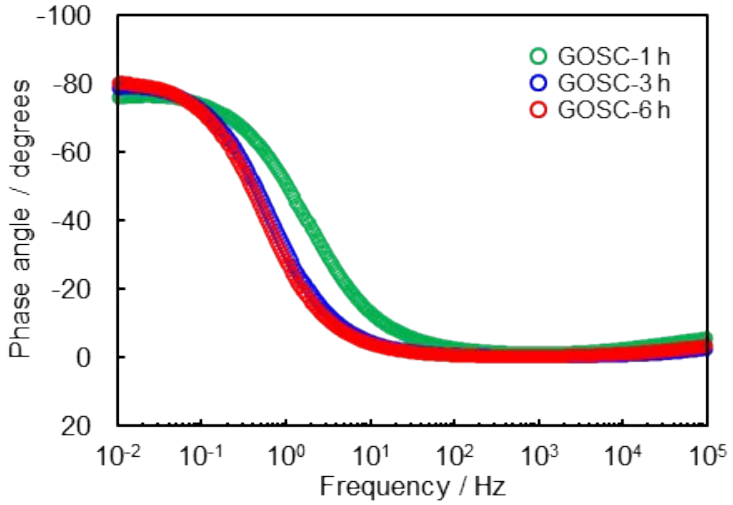

Figure S7. Impedance phase angle versus frequency for GOSC prepared using various photoreduction times. The corresponding time constant (τ_0) was calculated from $\tau_0 = 1/f_0$ (f_0: phase angle of −45°).

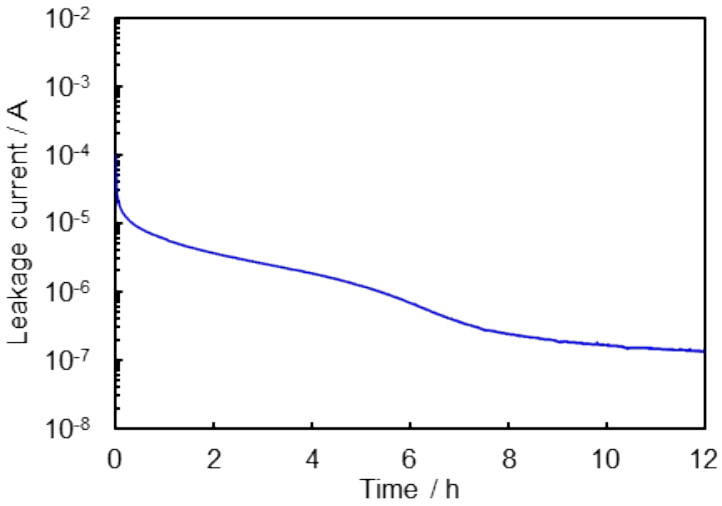

Figure S8. Leakage current measurement of GOSC-6 h. A DC voltage (the voltage at which the supercapacitor was operated, V_{max} = 1.0 V) was applied across GOSC-6 h device; the current required to retain this voltage was measured over a period of 12 h.[4]

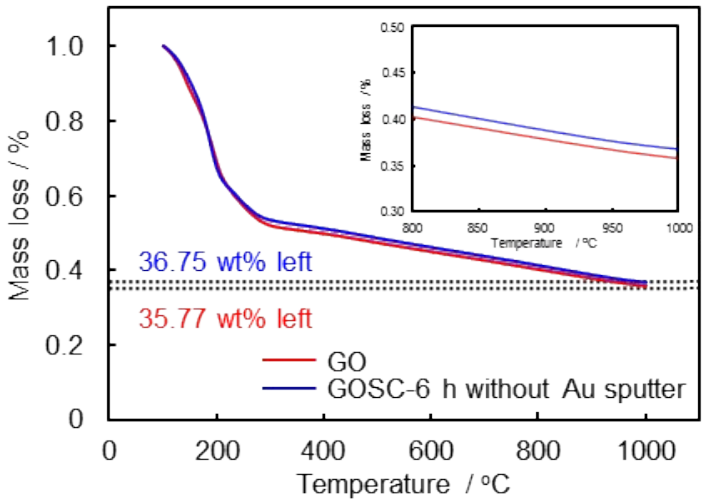

Figure S9. TGA plots of GO and GOSC-6 h without Au sputter. The mass of rGO active material for one electrode was calculated to be approximately 0.4 wt% of the total mass of GOSC-6 h without Au sputter (Details on calculation are given below in in Experimental section 6.2). However, the mass of the rGO active material is very small, as in the case of other micro-devices.[2,4,5] Therefore, we summarised the specific capacitance of GOSC based on the area of the rGO electrode.

Table S1. Summary of GOSC performance.

		Current (mA)	Capacitance (mF cm^{-2})	Capacitance (mF cm^{-3})	Power density (W cm^{-3})	Energy density (Wh cm^{-3})
GOSC-0 h	CV	-	0.01	-	-	-
	CC	0.05	0.07	0.03	0.02	2.63×10^{-6}
		0.1	0.06	0.02	0.01	1.79×10^{-6}
		0.5	-	-	-	-
GOSC-1 h	CV	-	0.39	-	-	-
	CC	0.05	0.44	0.18	0.06	2.09×10^{-5}
		0.1	0.35	0.14	0.04	1.35×10^{-5}
		0.5	-	-	-	-
GOSC-3 h	CV	-	0.83	-	-	-
	CC	0.05	0.82	0.33	0.13	4.25×10^{-5}
		0.1	0.69	0.28	0.13	3.38×10^{-5}
		0.5	0.56	0.23	0.09	1.64×10^{-5}
GOSC-6 h	CV	-	1.00	-	-	-
	CC	0.05	2.07	0.83	0.12	1.06×10^{-4}
		0.1	1.74	0.70	0.13	8.47×10^{-5}
		0.5	1.30	0.52	0.13	4.38×10^{-5}

Note: The volumetric stack capacitance (F cm^{-3}) of GOSC was calculated with the volume of the device taken into account, including the rGO, GO and Au current collector.

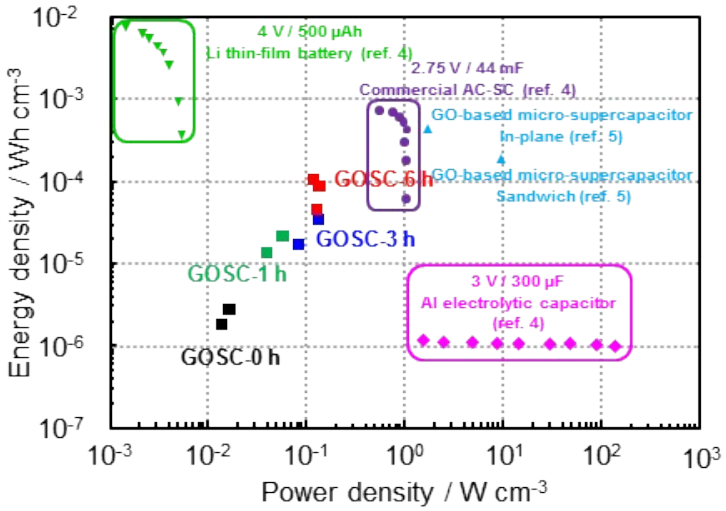

Figure S10. Comparative Ragone plot of a Li thin film battery,[4] commercial supercapacitor,[4] Al electrolytic capacitor,[4] GO-based micro-supercapacitor[5] and GOSC.

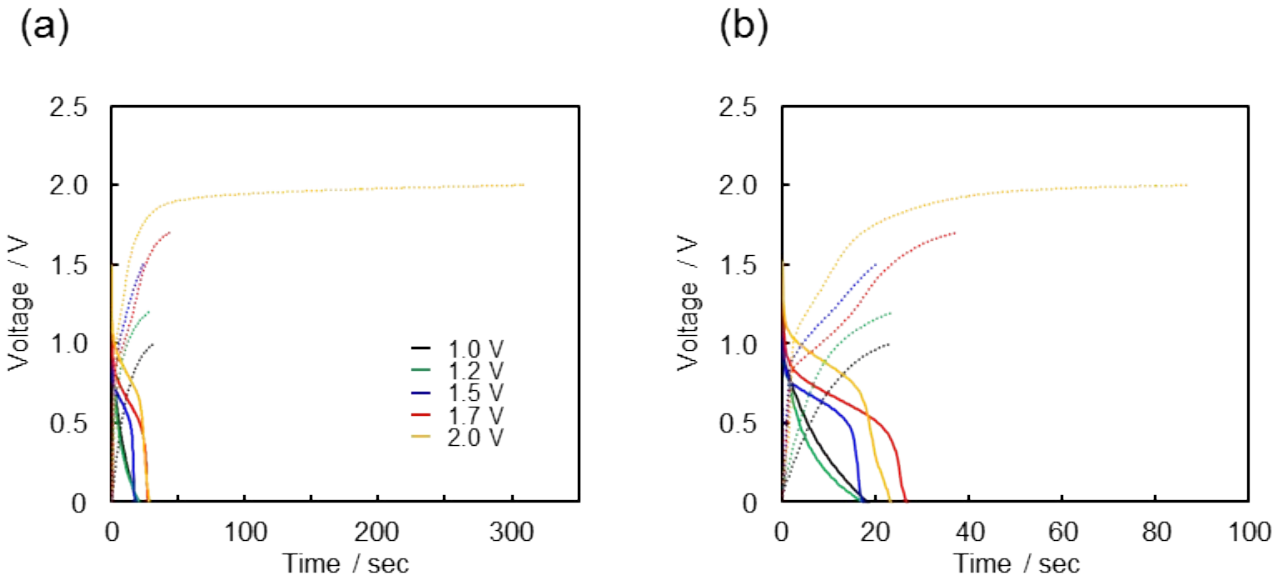

Figure S11. Galvanostatic charge/discharge curves of the rGO/GO/rGO device charged to various voltages at a current density of 0.05 mA cm^{-2}: (a) 1st cycle and (b) 5th cycle.

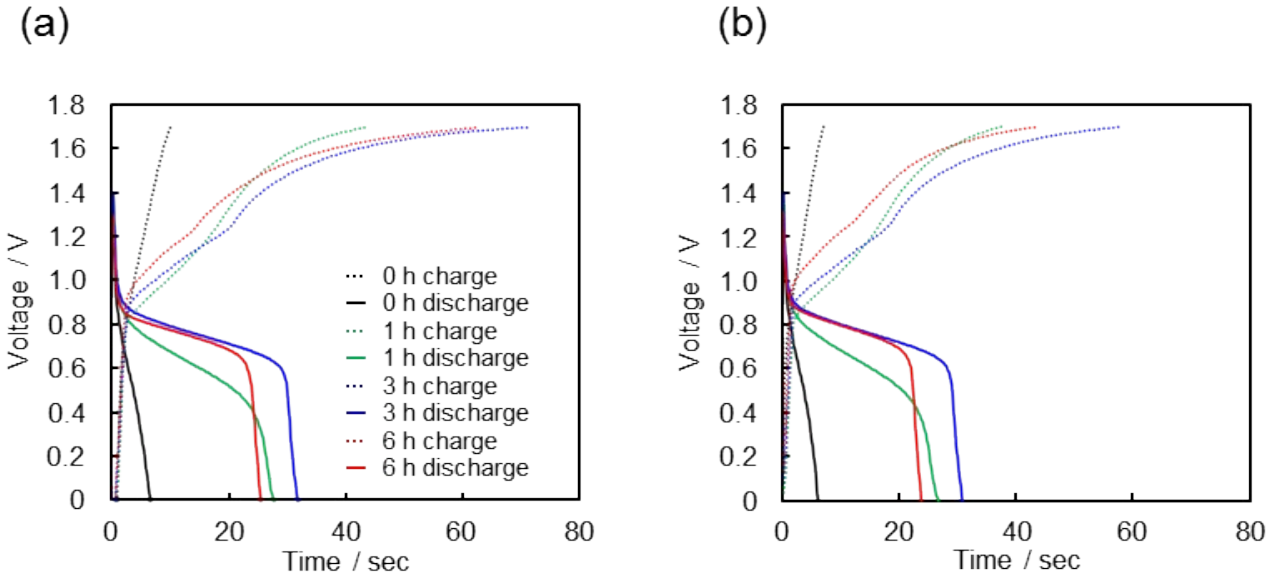

Figure S12. Galvanostatic charge/discharge curves of GORB prepared using various photoreduction times at a current density of 0.05 mA cm^{-2}: (a) 1st cycle and (b) 5th cycle.

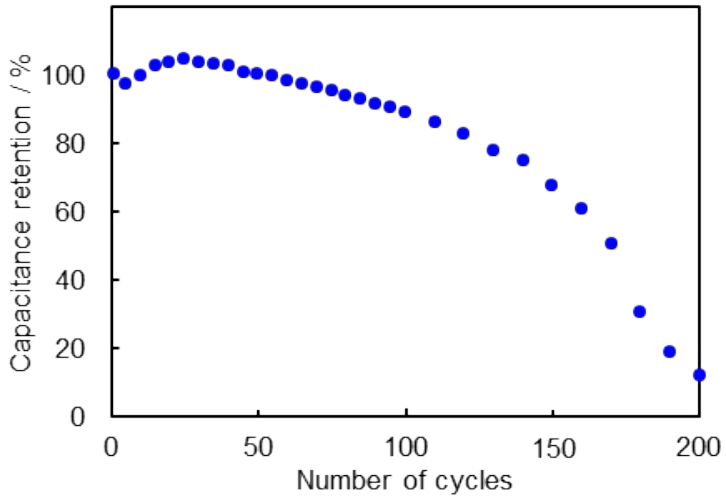

Figure S13. Cycle stability of GORB-3 h at 0.05 mA. Capacitance degradation was observed in GORB-3 h after 200 charge/discharge cycles. According to XPS analysis (Fig. S14), decreases in the oxygenated functional groups and increases in the CH defects of rGO anode were observed after 200 charge/discharge cycles. On the other hand, XPS spectra of the rGO cathode were barely changed. Thus, in the case of our GORB, we speculate that the main reasons of capacitance degradation were (1) decreasing the redox site of the rGO anode and (2) decreasing electron conductivity of the rGO anode derived increasing from CH defects.

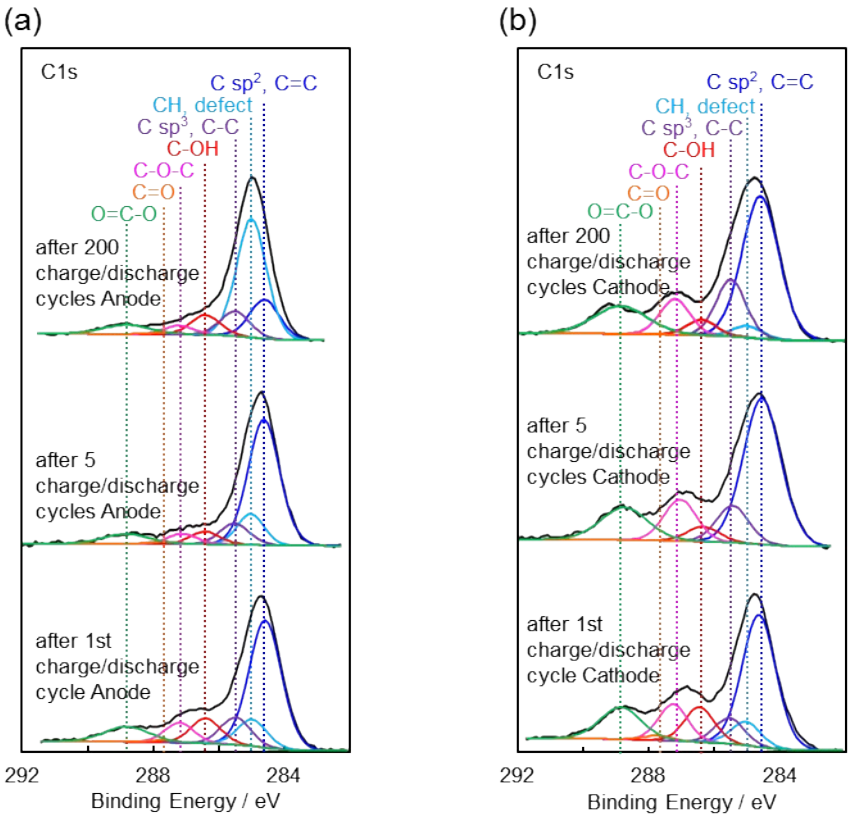

Figure S14. C 1s XPS spectra of (a) anode and (b) cathode of GORB-3 h after various charge/discharge cycles.

References

1 M. Koinuma, C. Ogata, Y. Kamei, K. Hatakeyama, H. Tateishi, Y. Watanabe, T. Taniguchi, K. Gezuhara, S. Hayami, A. Funatsu, M. Sakata, Y. Kuwahara, S. Kurihara and Y. Matsumoto, *J. Phys. Chem. C*, 2012, **116**, 19822-19827.

2 Q. Zhang, K. Scrafford, M. Li, Z. Cao, Z. Xia, P. M. Ajayan, and B. Wei, *Nano Lett.*, 2014, **14**, 1938-1943.

3 M. Koinuma, H. Tateishi, K. Hatakeyama, S. Miyamoto, C. Ogata, A. Funatsu, T. Taniguchi, Y. Matsumoto, *Chem. Lett.* 2013, **42**, 924-926.

4 M. F. El-Kady and R. B. Kaner, *Nat. Commun.*, 2013, **4**, 1475.

5 W. Gao, N. Singh, L. Song, Z. Liu, A. L. M. Reddy, L. Ci, R. Vajtai, Q. Zhang, B. Wei, and P. M. Ajayan, *Nat. Nanotechnol.*, 2011, **6**, 496-500.